High-T_c Ramp-Type Josephson Junctions with $PrBa_2Cu_{3-x}Ga_xO_{7-\delta}$ barrier

H. ROGALLA, M.A.J. VERHOEVEN, G.K. VAN ANCUM, D.H.A. BLANK AND G. GERRITSMA

University of Twente, P.O.Box 217, 7500AE Enschede, the Netherlands

INTRODUCTION

Superconducting three terminal devices [1] of sufficient current and voltage gain and integrability are not yet available, so Josephson junctions are still the basic active elements in superconducting electronics. In recent years a lot of effort has been put into the development of reproducible high-T_c Josephson junctions - with mixed success. Even though Josephson behaviour can easily be demonstrated in very simple configurations, the fabrication of reproducible junctions is still quite a problem and is not yet sufficient for medium or large scale levels of integration. Apart from a lack of the understanding of the basic mechanisms of high-T_c superconductivity, also the charge transport properties in high-T_c Josephson junctions are not yet fully understood. This, together with the extremely short coherence length of the order of the chemical binding length and the difficulties in preparing these materials, resulted in junction realisations that were quite often intrinsically complicated and not well understood in their physical behaviour but showed reasonably good current-voltage characteristics, e.g. the different types of grain boundary junctions [2]. In contrast, junctions with simple artificial barriers like normal conductor barriers made of Ag between $YBa_2Cu_3O_{7-\delta}$ show a quite reproducible behaviour if the interface between $YBa_2Cu_3O_{7-\delta}$ and the barrier is reasonably clean [3]. Due to the SNS characteristics and the low normal resistance of these junctions they are only useful for a very limited number of applications.

In other junctions with artificial barriers, like ramp-type junctions or planar junctions using a-axis [4] or 103-oriented electrodes and barriers [5], the barriers are grown epitaxially onto the $YBa_2Cu_3O_{7-\delta}$ electrodes and vice versa. The charge transport through such barrier materials (e.g., $PrBa_2Cu_{3-x}Ga_xO_{7-\delta}$, $SrRuO_4$ and $CaRuO_4$) has not been studied sufficiently in the past to reasonably well explain and predict the electrical properties of such junctions. This article will deal with preparation issues of $YBa_2Cu_3O_{7-\delta}$ ramp-type junctions with Ga-doped $PrBa_2Cu_3O_{7-\delta}$ barriers and the charge transport in such junctions.

RAMP-TYPE JUNCTION PREPARATION

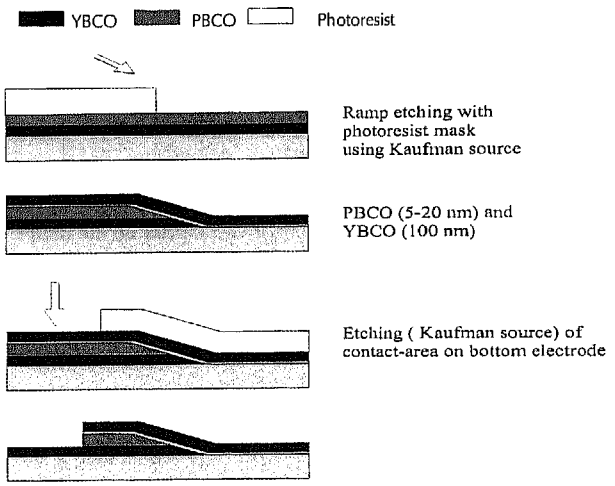

Figure 1: Steps in the fabrication of ramp-type junctions

The details of the process have been described elsewhere [6]. In short (see figure 1): In the first step an epitaxial bilayer of the superconductor (e.g. $YBa_2Cu_3O_{7-\delta}$) and a semiconductor or insulator (e.g. $PrBa_2Cu_3O_{7-\delta}$) are deposited. Next a photoresist mask is brought on and the ramp is structured into the film by an Ar ion-beam under 45° incident angle. After removal of the mask and cleaning of the ramp by an Ar ion-beam, the barrier layer (e.g. $PrBa_2Cu_3O_{7-\delta}$) and the counter electrode (e.g. $YBa_2Cu_3O_{7-\delta}$) are deposited. In the following etching step the overlap in the junction area is largely removed. Finally gold contacts are deposited using lift-off structuring.

A very critical step in this process is the formation of the ramp and the necessary cleaning of its surface prior to the deposition of the barrier and counter electrode if these steps are performed ex-situ. The cleaning process and the growth of a $PrBa_2Cu_3O_{7-\delta}$ barrier were studied in more detail in [7,8]. The damage of the ramp interface caused by the Ar ion-beam cleaning procedure was found to be very dependent on the acceleration voltage. Test junctions (ramp junctions without barrier) showed clear weak-link behaviour for high cleaning energies (500eV and 200eV ions). Their critical current density was reduced by one order of magnitude compared to the undisturbed film values. If cleaned with 50eV Ar ions, no weak link behaviour was observed and the critical current density was found to be very close to one of the thin film. In figure 2 the critical current density of ramp junctions with different $PrBa_2Cu_3O_{7-\delta}$ barrier thickness are plotted as function of the temperature .

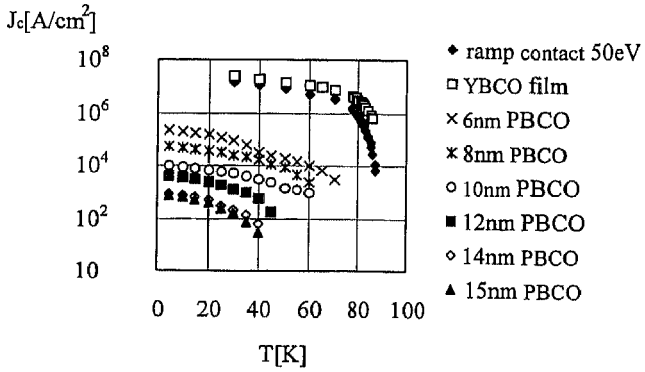

Figure 2: $J_c(T)$ of junctions with different $PrBa_2Cu_3O_{7-\delta}$ barrier thickness, of a 50eV cleaned test junction and of a bare film.

$J_c(T)$ decreases exponentially with the barrier thickness, at least starting from a barrier thickness of 6nm. In all cases, $J_c(T)$ falls off linearly roughly up to 40K and becomes parabolic at high temperatures. In prior studies [7] it has been shown by AFM measurements along the ramp that the $PrBa_2Cu_3O_{7-\delta}$ barrier grows in islands thus increasing its roughness drastically, before finally an island coalescence takes place at a barrier thickness of about 8nm. This effect can clearly be seen in figure 3, where an AFM measurement across a ramp with and without barrier is shown.

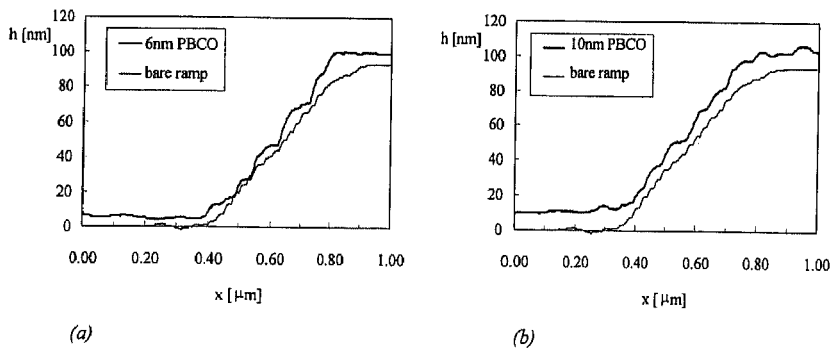

Figure 3: Cross-sections of a bare ramp covered with (a) 6nm PBCO and (b) 10nm PBCO, as obtained by AFM measurements.

The measurements presented in this section show that the barrier cleaning is essential in obtaining high quality ramp-type junctions. Good sample cooling and low Ar ion-energies are key ingredients. Nevertheless, a barrier thickness of at least 6nm..10nm has to be applied due to the island growth of the $PrBa_2Cu_3O_{7-\delta}$ barrier on the ramps. For a thickness of less than 6nm, the $PrBa_2Cu_3O_{7-\delta}$ barriers are surely leaking.

ELECTRONIC TRANSPORT IN $PrBa_2Cu_3O_{7-\delta}$

In order to understand the transport properties of $PrBa_2Cu_3O_{7-\delta}$ in more detail we studied its temperature dependent electric conductance in thin films of high-quality $PrBa_2Cu_3O_{7-\delta}$ with and without magnetic field and for low and high electric fields. Details of these measurements have been described elsewhere [9,10]. Here we include a short summary of the results which could be of relevance for the charge transport characteristics of ramp-type junctions with $PrBa_2Cu_3O_{7-\delta}$ barriers.

Thin films of fully c-axis oriented $PrBa_2Cu_3O_{7-\delta}$ with a typical thickness of 60nm were prepared on $SrTiO_3$ single crystal substrates by sputtering or laser ablation. The specific resistance of these films typically ranges from about $10^{-4}\Omega$cm at room temperature to $10^{1}\Omega$cm at 8K. For the films under investigation this means that resistance values of up to some 10GΩ have to be measured at low temperatures (down to 3.5K in the current measurement set-up). Reliable contacts to the films are essential and also the knowledge of their temperature dependent contact resistance. Therefor we applied the Transmission Line Model (TLM) method [11] which allows to determine the contact resistivity and film resistivity independently from each other. The lowest and least temperature dependant contact resistivity for ex-situ contact deposition was found for gold contacts with a value of about $10^{-8}\Omega$m at room temperature and $10^{-3}\Omega$m at 11K. The TLM structure with a length of 2685μm and a width of 300μm was etched into the film using wet chemical etching instead of Ar-plasma or ion-beam etching in order to minimise damage to the film and to avoid contamination of the $SrTiO_4$ substrate which could lead to a resistivity of the substrate comparable to that of the film under investigation.

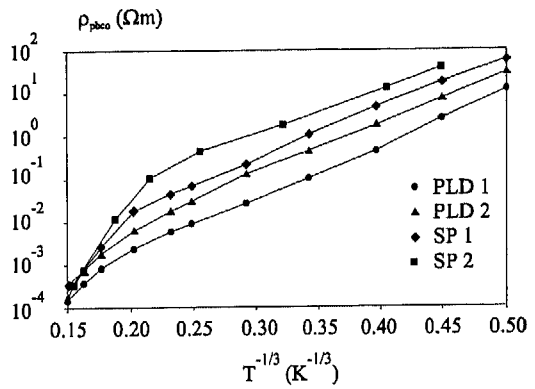

Figure 4: Semi-logarithmic plot of the $PrBa_2Cu_3O_{7-\delta}$ resistivity ρ_{pbco} as function of $T^{-1/3}$. PLD indicates films deposited by laser ablation, SP films deposited by sputtering.

The temperature dependence of the resistivity of laser ablated as well as the sputtered $PrBa_2Cu_3O_{7-\delta}$ films can well be explained by a 2D Mott variable-range hopping (VRH) model [12] for temperatures below 100K. The 2D Mott VRH model predicts a $T^{-1/3}$ temperature dependence of the resistivity (see figure 4). Oxygen annealing experiments show that the CuO-plain resistivity increases below 100K much faster than the chain resistivity, so that the film resistivity in the a-b plane is predominantly determined by the chain resistivity in the interesting temperature range (100K and below).

A further important signature for the 2D VRH is the dependence of the film's resistivity on the applied magnetic field H for fixed temperature (or equivalently its magnetoresistance $\rho(H)/\rho(0)$ for fixed T) [13]. One can distinguish two characteristic regions for the magnetoresistance,

a weak-field regime: $\left.\frac{\rho(H)}{\rho(0)}\right|_{weak} \propto \exp\frac{H^2}{k_B T}$ and

a strong-field regime: $\left.\frac{\rho(H)}{\rho(0)}\right|_{strong} \propto \exp\sqrt{\frac{H}{k_B T}}$.

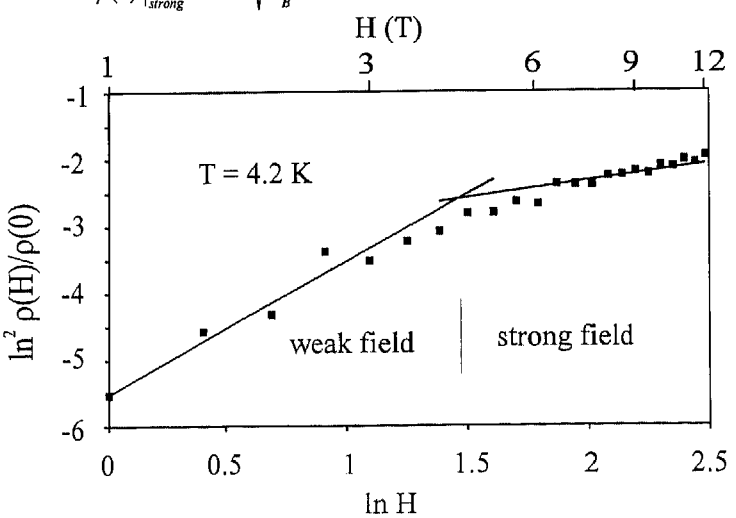

Figure 5: Magnetoresistance at 4.2K of a thin $PrBa_2Cu_3O_{7-\delta}$ film. The lines represent weak- and strong-field dependencies, as indicated.

Measurements of the magnetoresistance on thin c-axis oriented $PrBa_2Cu_3O_{7-\delta}$ films were performed at different temperatures and fields, with fields applied along the c-axis. For a typical film the magnetoresistance at 4.2K is plotted up to a field of 12T in figure 5. Clearly a weak and strong filed regime can be distinguished, with a transition between these regimes at a field of about 4.5T.

The measurements of the temperature dependence and magnetic field dependence of the resistivity of thin c-axis oriented $PrBa_2Cu_3O_{7-\delta}$ films described above are very strong evidence that these films are 2-D Mott variable-range hopping conductors. Whereas the temperature activation in general acts isotropically, fields (e.g. an electrical field) can activate VRH in specific directions. Activation by an electrical field is especially very pronounced at low temperatures when the thermal activation energy kT is small compared to the electrical activation energy $e\,\varepsilon_r\,E\,r(T,E)$, where e is the electron charge, ε_r the relative dielectric constant, E the applied electrical field and r(T,E) the energy and temperature dependent hopping distance in direction of E. This can be clearly seen in figure 6 where the resistivity of a $PrBa_2Cu_3O_{7-\delta}$ film is plotted as function of the applied electrical Field for different temperatures.

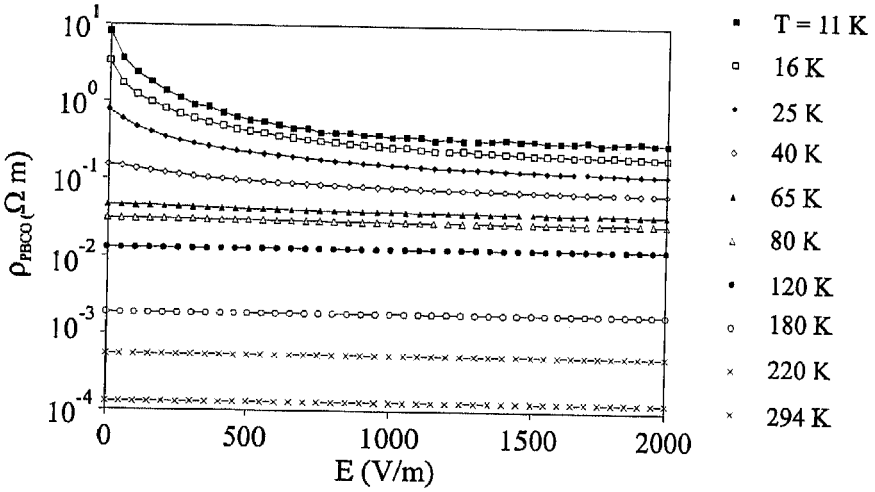

Figure 6: Resistivity ρ_{pbco} as function of the applied electrical field E at various temperatures T

If the electrical field is applied by the voltage source for measuring the resistivity of the film, the film resistivity in direction of the applied field can be written as [9,14] where the subscript x denotes the direction of the applied field:

$$\rho_{pbco,x}(T,E) = \rho_{0,x} \cdot \exp\left(\left[\frac{k_B T_0}{k_B T + e\varepsilon_r E_x r_x(T,E)}\right]^{1/3}\right)$$

Since all quantities apart from the hopping distance r_x can be measured this equation yields a tool to determine the mean hopping distance in the direction of the charge transport:

$$r_x(T,E) = \frac{k_B}{e\varepsilon_r E}\left(\frac{T_0}{\left[\ln\left(\rho(T,E)/\rho_0\right)\right]^3} - T\right)$$

Evaluating the data from figure 6 for the mean hopping distance, the dependence of the hopping distance on T and E is plotted in figure 7. It should be noted that the increase of the field activated hopping distance only takes place in the direction of the applied field. In the y- and z-direction the average hopping distance is essentially equal to the zero-field value in the x-direction. For E<200V/m the values for r_x are less accurate because of the dominance of the thermal activation in this regime.

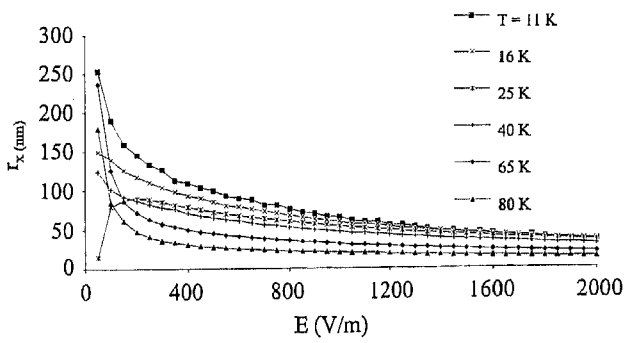

Figure 7: Resistivity ρ_{pbco} as function of the applied electrical field E at various temperatures T

In figure 7 it can be seen that the average hopping distance in the direction of the applied field tends towards a constant minimum of about 14nm. For other films values of the same order of magnitude were found. This minimum hopping distance can be interpreted as nearest neighbour hopping between localised states. The obtained value of 14nm is comparable to the estimate in literature of a nearest-neighbour distance of 10nm [15]. If we assume intrinsic localised states, only an estimated 3% of the Pr atoms provide a localised state. This argument agrees with a mixed valence state of the Pr atoms, where most Pr atoms are trivalent and only a minority is tetravalent with a localised hole in their vicinity.

CHARGE TRANSPORT IN $PrBa_2Cu_{3-x}Ga_xO_{7-\delta}$ RAMP-TYPE JUNCTIONS

As already lined out above, the ramp structuring and cleaning are essential steps in the fabrication of high-quality ramp type junctions. These enhancements are also visible in the charge transport characteristics of ramp-type junctions. Details will be published elsewhere [16], here a short summary of recent findings.
In contrast to earlier measurements improved ramp-type junctions show a much steeper dependence of the critical current density J_c as function of the barrier thickness t, leading to a decay length $\xi = d \ln J_c / dt \approx 1.7nm$ (see figure 8). This value is much more what one expected it to be, in contrast to earlier measurements, where values of 5nm to 8nm were found, probably due to insufficiently cleaned ramp surfaces and rough barriers. As can be seen from figure 8, the value of J_c is not dependent on the temperature between 4.2K and 45K.

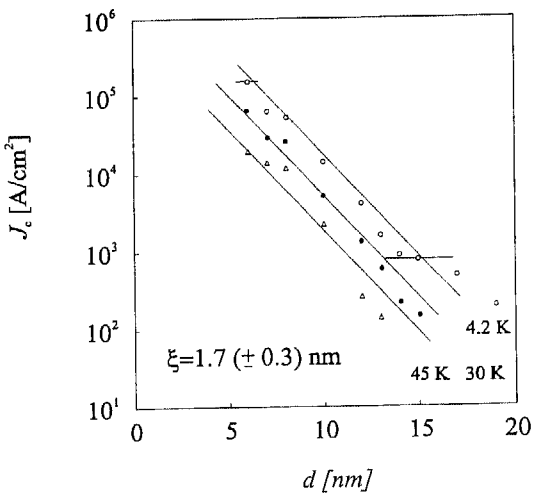

Figure 8: Critical current density as a function of the $PrBa_2Cu_3O_{7-\delta}$ thickness at T=4.2K, 30K and 45K.

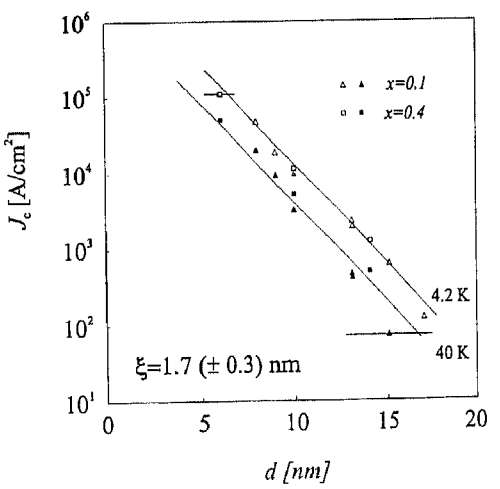

Figure 9: Critical current density as a function of the $PrBa_2Cu_{3-x}Ga_xO_{7-\delta}$ barrier thickness for x=0.1 and 0.4 at 4.2K and 40K.

Besides an adjustment of the critical current density of the junctions by changing the barrier thickness, also the resistance of the barrier can be changed. Doping with Y reduces the resistance [17] while doping with Ga increases its resistance [18]. It is known that Ga substitutes for copper in $PrBa_2Cu_3O_{7-\delta}$ on the chain sites [19]. This is chemically equivalent to oxygen depletion and leads to strong increases of the resistivity. Ramp-type junctions with a doping level of x=0.1 and x=0.4 of the $PrBa_2Cu_{3-x}Ga_xO_{7-\delta}$ barrier and different barrier thickness have been prepared. The dependence of their critical current density on the barrier thickness is shown in figure 9 for two temperatures.

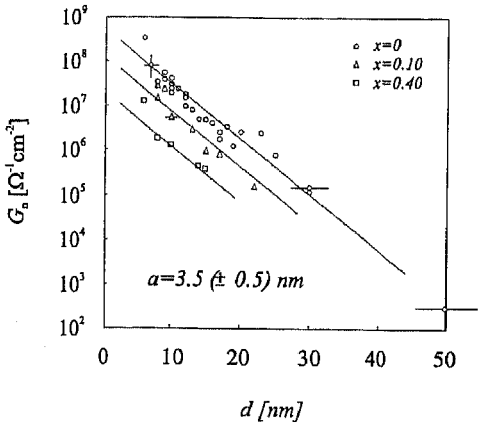

Figure 10: Zero-bias conductance at 4.2K as a function of the $PrBa_2Cu_{3-x}Ga_xO_{7-\delta}$ barrier thickness, for x=0, 0.1 and 0.4 .

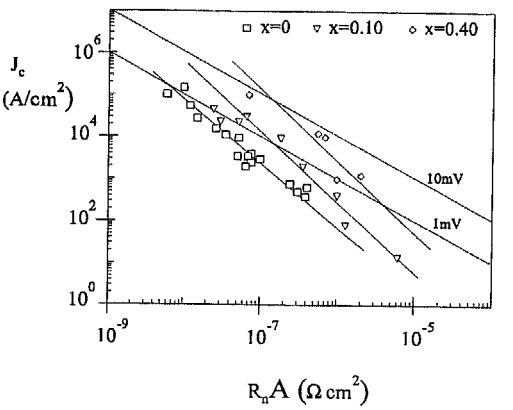

Figure 11: Plot of Jc as function of Rn×A. Lines of constant Ic×Rn-product are included.

Again a temperature independent decay length of 1.7nm is found. Additionally it can be seen that Jc is independent of the doping level and thus also the decay length. With this small value of ξ and its temperature independence, a direct tunnelling process for the superconducting charge carriers through the barrier becomes very likely.
In contrast to the independence of J_c on the doping level, the normal state conductance G_n is strongly dependent on the doping (see figure 10). Doping with x=0.4 decreases G_n by nearly two orders of magnitude. The normal decay length a is independent of the doping and about twice as large as ξ: a = 3.5nm . This means that there are two distinct tunnelling channels for superconducting charges and normal conducting charges. Superconducting charges tunnel through the barrier directly while normal conducting charges seem to tunnel via one intermediate state.
As a consequence, J_c and the normal conducting resistance can be adjusted independently. The first one by the barrier thickness, the second one by Ga-doping. Also the $I_c{\cdot}R_n$-product can strongly be influenced by the doping. In figure 11 the critical current density J_c is plotted as function of $R_n{\cdot}A$ and lines of constant $I_c{\cdot}R_n$-product are added. Obviously doping with Ga shifts the curves towards higher $I_c{\cdot}R_n$-products while keeping J_c constant. Further enhancing the resistance of the normal conducting transport channel would decrease the shunting of the superconducting channel and thus would further increase the $I_c{\cdot}R_n$-product and could make real tunnelling characteristics possible.

REFERENCES

1. see e.g., Mannhart J (1995) Superconductor Science and Technology 8, 1-19
2. Gross R, Alff L, Beck A, Fröhlich OM, Gerber R, Gerdemann R, Marx A, Mayer B and Koelle D (1995) Proceedings of the 2nd Workshop on HTS Appl. and New Materials. Twente University, Netherlands, pp 8-15
3. Ono RH, Vale LR, Kimminau KR, Beall JA, Cromar MW, Reintsma CD, Hravey TE, Rosenthal PA and Rudmen DA (1993) IEEE Trans. Appl. Superconductivity 3: 2389
4. Barner JB, Rogers CT, Inam A, Ramesh R and Bersey S (1991) Appl.Phys.Lett. 59: 742
5. Akoh H, Sato H, and Takada S (1995) IEEE Trans. Appl. Superconductivity 5: 2373
6. Terpstra D, Rijnders AJHM, Roesthuis FJG, Blank DHA, Gerritsma GJ and Rogalla H (1993) J. of Alloys and Compounds 195: 719
7. Verhoeven MAJ, Moerman R, Bijlsma ME, Rijnders AJHM, Blank DHA, Gerritsma GJ and Rogalla H (1995) submitted to Appl.Phys.Letters
8. Verhoeven MAJ, Gerritsma GJ and Rogalla H (1995) Proceedings EUCAS 95
9. van Ancum GK, Verhoeven MAJ, Blank DHA and Rogalla H (1995) Phys.Rev. B52: 5598
10. van Ancum GK, Verhoeven MAJ, Blank DHA and Rogalla H (1995) Phys.Rev. B52: 5644
11. Berger HH (1972) Solid State Electron. 15: 145
12. Mott NF and Davis EA (1979) Electronic Processes in Non-Crystalline Materials. Clarendon. Oxford.
13. see e.g., Shklovskii BI and Efros AL (1984) Electronic Prop. of Doped Semiconductors. Springer Verlag.Berlin.
14. van Ancum GK (1996) Electronic Transport Properties of $PrBa_2Cu_3O_{7-\delta}$. Thesis. UTwente, the Netherlands.
15. Kabasawa U, Tarutani Y, Fukazawa T, Hiratani M and Takagi K (1993) Phys.Rev.Lett. 70: 1700
16. Verhoeven MAJ, Gerritsma GJ and Rogalla H (1995) submitted to Phys.Rev.Letters
17. Radousky HD (1992) J.Mater.Res. 7: 1917
18. Xu Y and Guan W (1993) Physica C 206: 59
19. Xiao G (1988) Nature 332: 238